RESEARCH ARTICLE

A Study of Removal of Lead (II) Ions from Aqueous Solution on Chitosan-g-poly (acrylic acid-co-crotonic acid) Hydrogel

Rasha A. Mohammed,[1] Hazim A. Walli[2*]

[1]Department of Chemistry, College of Education, University of Al-Qadisiyah, Diwaniya, Iraq
[2]Department of Ecology, College of Science, University of Al-Qadisiyah, Diwaniya, Iraq

Received: 10th October, 2022; Revised: 17th November, 2022; Accepted: 10th December, 2022; Available Online: 25th December, 2022

ABSTRACT

This study used chitosan-g-poly (acrylic acid-co-crotonic acid) hydrogel (Ch-g-P(AA-CA)) as an adsorbent to remove aqueous solutions of lead ion (Pb (II)). A flame atomic absorption spectrophotometer was used to estimate the ion's adsorption amounts. Metal ion concentration, pH, existing salt, and temperature were all studied. A gile's classification indicates that these isotherms are of the L-curve type, and the experimental data were best fit by Langmuir and Freundlich isotherm models. At various temperatures (15, 20, 25, and 30°C), adsorption and various thermodynamic parameters (ΔH, ΔS, and ΔG) were studied. It was found that the adsorption process was not spontaneous, based on the thermodynamic parameters of the metal ion-ch-g-P(AA-CA) hydrogel systems. Ch-g-P(AA-CA) hydrogel adsorption increased as the pH of the solution rose and decreased as the ionic strength rose, according to the study's findings.

Keywords: Acrylic acid, Adsorption, Chitosan, Crotonic acid, Hydrogel, Pb (II) ions, Pollution, Thermodynamic.

International Journal of Drug Delivery Technology (2022); DOI: 10.25258/ijddt.12.4.59

How to cite this article: Mohammed RA, Walli HA, A Study of Removal of Lead (II) Ions from Aqueous Solution on Chitosan-g-poly (acrylic acid-co-crotonic acid) Hydrogel. International Journal of Drug Delivery Technology. 2022;12(4):1844-1848.

Source of support: Nil.

Conflict of interest: None

INTRODUCTION

Water pollution is a major environmental issue. Natural water sources are becoming more contaminated with metallic substances as a result of the increased use of the major 20 heavy metals.[1,2] On-site industrial wastewater testing has revealed the presence of high concentrations of toxic heavy metal ions. Many industries, such as metal plating, mining, and tanneries, have heavy metal contamination in their aqueous waste streams.[3,4] Copper, lead, cadmium, chromium, and mercury are just some of the heavy metal ions that pose a risk to human health. Heavy metals, which are not biodegradable and tend to accumulate in living organisms, can cause a variety of diseases and disorders.[5,6] Every lead compound is regarded as a toxic accumulator. The nervous system and gastrointestinal tract can be affected by acute lead poisoning. One of the 16th most toxic pollutants, chromium, has become a major public health issue because of its carcinogenic and teratogenic properties.[7] One method for removing high levels of heavy metals from water is the reduction process, which uses ferrous chloride as an oxidant, followed by a chelating resin, followed by biosorption.[8] Adsorption is a popular technique because of its simplicity and the wide variety of adsorbents available.[9-12] Adsorbents with lower costs are preferable to activated carbon because of their widespread use in water and wastewater treatment.[13] Many low-cost adsorbents, including bentonite clay, mango peel waste, wheat bran, olive oil waste, rice husk, and oil palm shell, have been treated to remove heavy metals.[14-16] This study aims to look into the ability of locally available Ch-g-P(AA-CA) hydrogel to remove lead ions from aqueous solution under various temperatures, pH, and ionic strength conditions, as well as to calculate the thermodynamic functions at equilibrium.

MATERIALS AND METHODOLOGY

Instruments

Atomic absorption spectrophotometer (AAS), Shimadzu. AA-6300, Japan, Shaker water bath, K&K Scientific, Korea, Centrifuge, CL008, Belgium, Electronic Balance, Sartorius Lab. L420 B, +0.0001g, pH-Meter, HM-73, TDA Electronic Ltd, Vortex, Hook and Tuker, Mst.Ltd., Gallenkamp.

Materials

Fluka provided hydrochloric acid and sodium chloride, while BDH provided lead nitrate. Himedia (India) provided the acrylic acid, acrylamide, acetic acid, and activated N,N,N', N'-tetra methyl ethylene diamine (TEMED), while (Fluka, Germany) provided the initiator KPS (potassium persulfate). N, N'-methylene bisacrylamide (NMBA) was purchased as a multifunctional crosslinker (Fluka, Germany).

*Author for Correspondence: layth.alhayder@gmail.com

METHODOLOGY

Preparation of Ch-g-P(AA-CA) hydrogel

Procedures for preparing a Ch-g P(AA-CA) from Ch, AA and CA were followed. Relatively small amounts (0.5 g) of Ch were added to 20 mL of acetic acid solution (1%) and mechanically stirred for 30 minutes. A reflux condenser, funnel, and nitrogen line was also used. A 5 mL of AA and 0.5 g in 5 mL CA were added to the solution after it had been purged with nitrogen for 30 minutes to remove any oxygen dissolved in the system. The solution was then heated to 60°C. MBA (0.05 g in 2 mL) and KPS (0.05 g in 2 mL) have recently been added to the flask. For three hours, the water bath was kept at 60°C. After that, they were baked at 70°C until they reached a constant weight. All of the test samples were milled to a particle size of 200 mesh or smaller. Ch-g-P(AA-CA) was made in the same way.

Preparation of Hydrogel

Ch-g-P(AA-CA) hydrogel in powder form was washed with a lot of distilled water, and it was washed several times to get rid of dust and soluble materials. The powder was baked at 120°C for 24 hours before being stored in airtight containers. The surface of the hydrogel was ground and sieved down to a particle size of 75 mm.

Adsorption Isotherm

There was 0.05 g of hydrogel in stoppered flasks when metal ions solutions 10 mL were added. The flasks were shaken in a temperature-controlled incubator at a speed of 120 rpm for 120 minutes until equilibrium was reached for Pb (II). The adsorption process reaches equilibrium in each of these cases within these times. It took about 20 minutes to centrifuge the suspensions at 3000 rpm after they reached equilibrium. AAS was used to analyze the metal content after the appropriate dilution of the clear supernatant. The data was compared against a calibration curve to determine the equilibrium concentrations.[17]

The following equation was used to determine the amount of metal adsorbed:

$$Q = \frac{V(C_o - C_e)}{m} \qquad (1)$$

Where m adsorbent weight (g), solution volume (L), concentrations (mg/L) Co and Ce represent the initial and equilibrium concentrations of the adsorbent, respectively.

Effect of Temperature

To estimate the basic thermodynamic functions of the process, the adsorption experiment was repeated in the same way at different temperatures: 25, 40, and 55°C.

Effect of pH

As previously mentioned, adsorption experiments were carried out as a function of pH with a fixed concentration of metal ions. The pH was adjusted with hydrochloric acid and sodium hydroxide in the range of 2 to 10. The pH of the suspensions was measured using a pH meter at the start and end of the experiment.

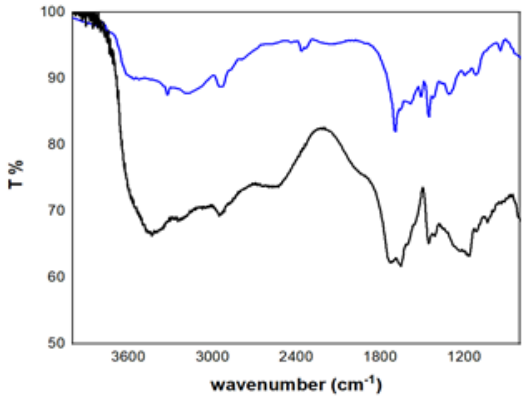

Figure 1: FTIR spectra of Ch-g-P(AA-CA) and Pb-Ch-g-P(AA-CA)

RESULTS AND DISCUSSION

Fourier-transform Infrared Spectroscopy (FTIR)

Characterization of hydrogels using FTIR was performed before and after the Pb(II) ions surface adsorption process (Figure 1). Ch-g-P(AA-CA) exhibits a markedly different adsorption intensity, and this difference is clearly discernible. Pre-adsorption hydrogels show an obvious decrease in the intensity of bands adjacent to the adsorption in the FTIR spectra. Because the Pb(II) ions is acidic, the adsorption process on these Pb(II) ions is weak, as demonstrated by this experiment. Acidic aggregates on the surface also cause a variation in absorption intensity.[18,19]

Field Emission Scanning Electron Microscopy (FESEM)

Before the adsorption process, the technique FESEM was used to determine the nature and porosity of the prepared surface, as well as the size and shape of the particles and the nature of their distribution. After the Pb (II) ions loading process, the surface became rougher and contained more cavities; after the adsorption process, the surface became rougher and contained more cavities. As shown in Figure 2, all the active sites on the Ch-g-P(AA-CA) surface were filled, indicating that the adsorption process had succeeded.[20]

Pb (II) equilibrium uptake onto Ch-g-P(AA-CA) hydrogel as a function of initial ion concentration at 25°C was shown in Figure 3. The relationship between equilibrium concentration

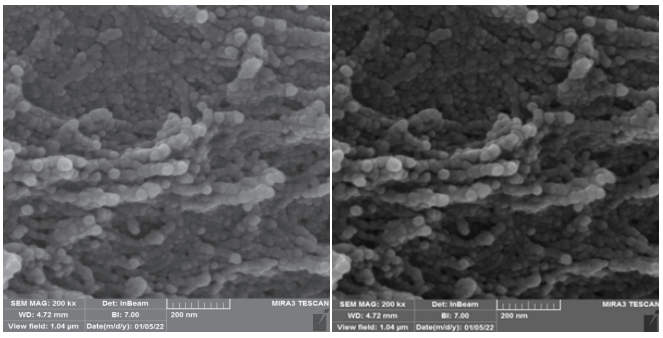

Figure 2: (a) SEM Image (500M) of Ch-g-P(AA-CA) image (b) Pb(II) loading on Ch-g-P(AA-CA) image

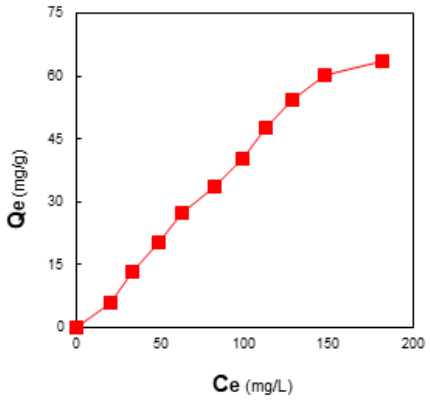

Figure 3: Adsorption isotherms of Pb (II) ions on Ch-g-P(AA-CA) hydrogel at 25°C

and adsorption capacity (Qe) is shown in Figure 3. As the concentration increased, so did the adsorption capacity.

The shapes of metal ions isotherms can be considered as L-type according to Giles classification. At the adsorption sites, the L-type indicates a much stronger interaction between sorbate and sorbent than between solvent and sorbent. Amide, carboxyl and hydroxyl groups in the Ch-g-P(AA-CA) hydrogel cell wall may be responsible for tying up metal ions. Metal ions replaced hydrogen ions in these groups as a result of the biosorption.[21-23]

Chemically, adsorption isotherms describe how metal ions are removed from a solution. Using the Langmuir, Freundlich, and Temkin models to describe adsorption isotherm data is common. The linear plot of Langmuir, Freundlich, and Temkin models shows that the adsorption of Pb(II) ions onto Ch-g-P(AA-CA) hydrogel seems to follow the Langmuir model (Figure 4 and Table 1).

The value of Freundlich constants and correlation coefficient are presented in Table 1. The magnitude of n (n=0.938) shows favorable adsorption of onto Ch-g-P(AA-CA) hydrogel. As indicated by the value of the correlation coefficient (R^2 = 0.9810), the adsorption of Pb (II) onto Ch-g-P(AA-CA) hydrogel was not followed by the Freundlich isotherm.[24,25]

As can be seen in Figure 5, the general shapes of the metal ion adsorption isotherms at four different temperatures.

The results showed an increase in the amount of Pb (II) adsorbed onto Ch-g-P(AA-CA) hydrogel with increasing temperature; hence the adsorption process appeared endothermic. Endothermic metal uptake can be attributed to the possibility that the metal ions are well-solvated in aqueous solutions, and the adsorption process requires appreciable energy.

The fundamental thermodynamic quantities of adsorption of metal ions onto Ch-g-P(AA-CA) hydrogel were estimated

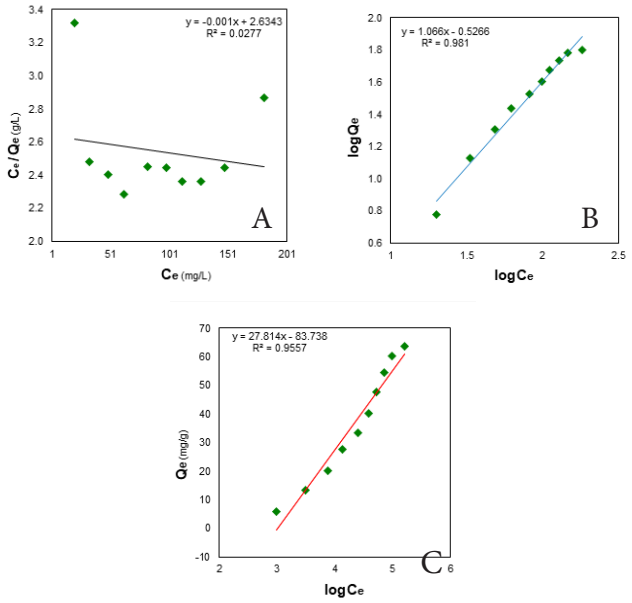

Figure 4: Modeling Pb (II) adsorption using Langmuir (A), Freundlich (B), and Temkin (C) adsorption models at 25oC

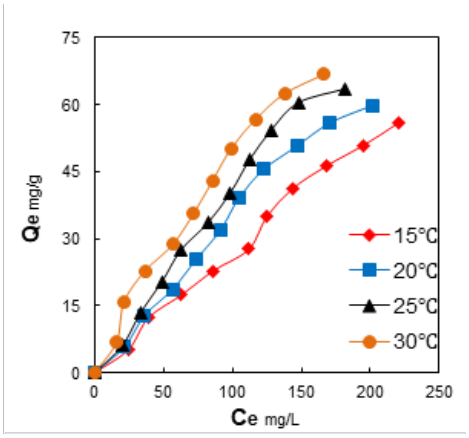

Figure 5: Adsorption isotherms of metal lead Ions onto Ch-g-P(AA-CA) hydrogel at different temperatures

by calculating X_m values at different temperatures. The heat of adsorption (ΔH) may be obtained from Van't Hoff equation: $ln\,X_m = \frac{-\Delta H}{RT} + cons.$, the change in free energy (ΔG) could be determined from equation ($\Delta G = -RTlnK$), and the change in entropy (ΔS) was calculated from Gibbs's equation: (ΔG=ΔH-T. ΔS). Table 2 and Figure 6 demonstrate these calculations.[26-28] Table 3 shows the basic thermodynamic values of the adsorption of metal ions on Ch-g-P(AA-CA) hydrogel. An adsorption of the van der Waals type is suggested to take place as indicated by these values.

The higher the ΔG value, the more likely the process is to be non-spontaneous. The decrease in randomness at the

Table 1: Freundlich and Langmuir isotherm constants for metals ions uptake by Ch-g-P(AA-CA) hydrogel

Metal ion	Langmuir model			Freundlich model			Temkin model		
	K_L	q_m	R^2	K_F	n	R^2	K_T	B	R^2
Pb (II)	0.001	500	0.3338	0.297	0.938	0.9810	0.049	0.4389	0.9557

Table 2: Effect of temperature on the maximum adsorbed quantity for adsorption of Metal ions onto Ch-g-P(AA-CA) hydrogel

T (°C)	T (K)	$1000/T\ K^{-1}$	*Pb(II)*	
			C_e =165	
			X_m	$ln\ X_m$
15	288	3.472	46.0	3.828
20	293	3.412	55.0	4.007
25	298	3.355	62.3	4.131
30	303	3.300	66.5	4.197

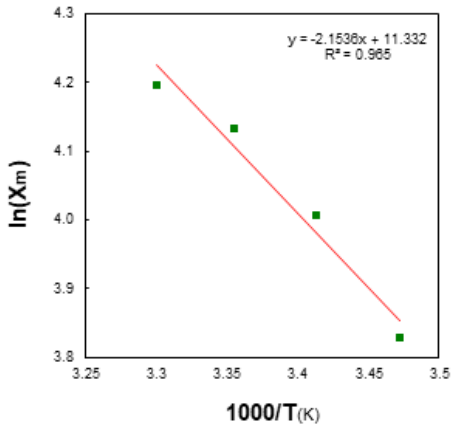

Figure 6: Plot of ln X_m against reciprocal absolute temperature for adsorption of metal ions onto Ch-g-P(AA-CA) hydrogel

Table 3: Values of thermodynamic functions of adsorption process of metal ions on Ch-g-P(AA-CA) hydrogel at 25°C

ΔH, $KJ.mol^{-1}$	ΔG, $KJ.mol^{-1}$	ΔS, $J\ mol^{-1}K^{-1}$	K_{eq}
17.905	7.800	33.908	0.800

solid-solution interface during ion fixation on the active sites of the adsorbent is revealed by the negative value of ΔS for metal ion adsorption.[29, 30] The percentage of ions removal by Ch-g-P(AA-CA) hydrogel has been found to be dependent on the pH of the solution (Figure 7), which increased with an increase in pH.

It's difficult to predict how metal ions will behave in an aqueous solution because they can exist in various forms and exhibit varying degrees of activity. Pb (II) ions in an aqueous solution exist at low pH. Insoluble metal hydroxides, such as $Pb(OH)^{+}$, are formed when the ions hydrolyze above pH 6.5. The adsorption of ions and metal ions on the exchangeable ion sites of the Ch-g-P(AA-CA) hydrogel is suppressed in an acidic pH because of the high concentration of H^{+} ions. Resulting in the suppression of ions adsorption on the exchangeable ion sites of Ch-g-P(AA-CA) hydrogel and metal ions adsorption decreases.[31-33]

CONCLUSIONS

Based on the experimental results of this investigation, the following conclusions can be drawn:

- Ch-g-P(AA-CA) hydrogel, as an adsorbent, can be used for the removal of Pb (II) ions from the solution.

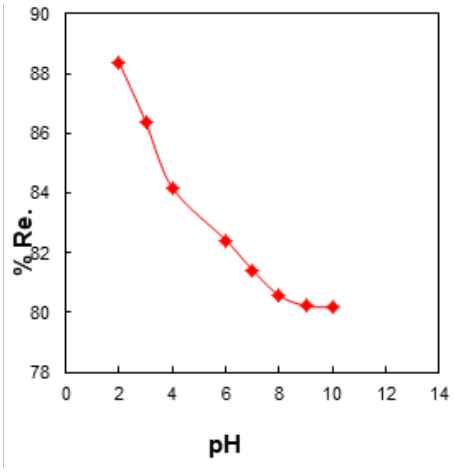

Figure 7: Effect of pH on the adsorption of Pb (II) ions onto Ch-g-P(AA-CA) hydrogel at 25°C

- The adsorption capacity of Ch-g-P(AA-CA) hydrogel was higher for Pb (II).
- Thermodynamic studies confirmed that the adsorption process of Pb (II) onto Ch-g-P(AA-CA) hydrogel was exothermic. The thermodynamic values of ΔG are positive for both systems, indicating a non-spontaneous process.
- The percentage removal of metal ions was dependent on the pH solution.

REFERENCES

1. Masindi V, Muedi KL. Environmental contamination by heavy metals. Heavy metals. 2018;10:115-32.
2. Rangel-Mendez JR, Monroy-Zepeda R, Leyva-Ramos E, Diaz-Flores PE, Shirai K. Chitosan selectivity for removing cadmium (II), copper (II), and lead (II) from aqueous phase: pH and organic matter effect. J Hazard Mater. 2009;162(1):503-11.
3. Zamora-Ledezma C, Negrete-Bolagay D, Figueroa F, Zamora-Ledezma E, Ni M, Alexis F, et al. Heavy metal water pollution: A fresh look about hazards, novel and conventional remediation methods. Environmental Technology & Innovation. 2021;22:101504.
4. Wang X, Sun R, Wang C. pH dependence and thermodynamics of Hg (II) adsorption onto chitosan-poly (vinyl alcohol) hydrogel adsorbent. Colloids Surf Physicochem Eng Aspects. 2014;441:51-8.
5. Kumar M, Seth A, Singh AK, Rajput MS, Sikandar M. Remediation strategies for heavy metals contaminated ecosystem: A review. Environmental and Sustainability Indicators. 2021;12:100155.
6. Kumar M, Tripathi BP, Shahi VK. Crosslinked chitosan/polyvinyl alcohol blend beads for removal and recovery of Cd (II) from wastewater. J Hazard Mater. 2009;172(2-3):1041-8.
7. Lv Q, Hu X, Zhang X, Huang L, Liu Z, Sun G. Highly efficient removal of trace metal ions by using poly (acrylic acid) hydrogel adsorbent. Materials & Design. 2019;181:107934.
8. Ajiboye TO, Oyewo OA, Onwudiwe DC. Conventional and Current Methods of Toxic Metals Removal from Water Using g-C3N4-Based Materials. Journal of Inorganic and Organometallic Polymers and Materials. 2021;31(4):1419-42.
9. Mahdi MA, Jasim LS, Ranjeh M, Masjedi-Arani M, Salavati-Niasari M. Improved pechini sol-gel fabrication of Li2B4O7/

NiO/Ni3(BO3)2 nanocomposites to advanced photocatalytic performance. Arabian Journal of Chemistry. 2022;15(5).
10. Singh S, Kumar V, Datta S, Dhanjal DS, Sharma K, Samuel J, et al. Current advancement and future prospect of biosorbents for bioremediation. Sci Total Environ. 2020;709:135895.
11. Mahdi MA, Yousefi SR, Jasim LS, Salavati-Niasari M. Green synthesis of DyBa2Fe3O7.988/DyFeO3 nanocomposites using almond extract with dual eco-friendly applications: Photocatalytic and antibacterial activities. Int J Hydrogen Energy. 2022.
12. Mahdi MA, Yousefi SR, Jasim LS, Salavati-Niasari M. Green synthesis of DyBa2Fe3O7.988/DyFeO3 nanocomposites using almond extract with dual eco-friendly applications: Photocatalytic and antibacterial activities. Int J Hydrogen Energy. 2022;47(31):14319-30.
13. Jasim LS, Aljeboree AM, Sahib IJ, Mahdi MA, Abdulrazzak FH, Alkaim AF, editors. Effective adsorptive removal of riboflavin (RF) over activated carbon. AIP Conf Proc; 2022.
14. Vardhan KH, Kumar PS, Panda RC. A review on heavy metal pollution, toxicity and remedial measures: Current trends and future perspectives. J Mol Liq. 2019;290:111197.
15. Tatarchuk T, Bououdina M, Al-Najar B, Bitra RB. Green and ecofriendly materials for the remediation of inorganic and organic pollutants in water. A new generation material graphene: Applications in water technology. 2019:69-110.
16. Ganduh SH, Aljeboree AM, Mahdi MA, Jasim LS. Spectrophotometric Determination of Metoclopramide-HCL in the Standard Raw and it Compared with Pharmaceuticals. Journal of Pharmaceutical Negative Results. 2021;12(2):44-8.
17. Mahdi MA, Aljeboree AM, Jasim LS, Alkaim AF. Synthesis, characterization and adsorption studies of a graphene oxide/polyacrylic acid nanocomposite hydrogel. NeuroQuantology. 2021;19(9):46-54.
18. Haider M, Hassan MA, Ahmed IS, Shamma R. Thermogelling platform for baicalin delivery for versatile biomedical applications. Mol Pharm. 2018;15(8):3478-88.
19. Irani M, Ismail H, Ahmad Z, Fan M. Synthesis of linear low-density polyethylene-g-poly (acrylic acid)-co-starch/organo-montmorillonite hydrogel composite as an adsorbent for removal of Pb (II) from aqueous solutions. Journal of Environmental Sciences. 2015;27:9-20.
20. Bashir S, Teo YY, Ramesh S, Ramesh K, Mushtaq MW. Rheological behavior of biodegradable N-succinyl chitosan-g-poly (acrylic acid) hydrogels and their applications as drug carrier and in vitro theophylline release. Int J Biol Macromol. 2018;117:454-66.
21. Abdulsahib WK, Sahib HH, Mahdi MA, Jasim LS. Adsorption Study of Cephalexin Monohydrate Drug in Solution on Poly (vinyl pyrrolidone-acryl amide) Hydrogel Surface. International Journal of Drug Delivery Technology. 2021;11(4):1169-72.
22. Xu X, Ouyang X-k, Yang L-Y. Adsorption of Pb (II) from aqueous solutions using crosslinked carboxylated chitosan/carboxylated nanocellulose hydrogel beads. J Mol Liq. 2021;322:114523.
23. Ngah WSW, Fatinathan S. Pb (II) biosorption using chitosan and chitosan derivatives beads: Equilibrium, ion exchange and mechanism studies. Journal of Environmental Sciences. 2010;22(3):338-46.
24. Yan H, Yang L, Yang Z, Yang H, Li A, Cheng R. Preparation of chitosan/poly (acrylic acid) magnetic composite microspheres and applications in the removal of copper (II) ions from aqueous solutions. J Hazard Mater. 2012;229:371-80.
25. Zhou Y, Fu S, Zhang L, Zhan H, Levit MV. Use of carboxylated cellulose nanofibrils-filled magnetic chitosan hydrogel beads as adsorbents for Pb (II). Carbohydr Polym. 2014;101:75-82.
26. Zhu Y, Zheng Y, Wang F, Wang A. Fabrication of magnetic macroporous chitosan-g-poly (acrylic acid) hydrogel for removal of Cd2+ and Pb2+. Int J Biol Macromol. 2016;93:483-92.
27. Shirsath SR, Patil AP, Patil R, Naik JB, Gogate PR, Sonawane SH. Removal of Brilliant Green from wastewater using conventional and ultrasonically prepared poly (acrylic acid) hydrogel loaded with kaolin clay: a comparative study. Ultrason Sonochem. 2013;20(3):914-23.
28. Nakhjiri MT, Marandi GB, Kurdtabar M. Poly (AA-co-VPA) hydrogel cross-linked with N-maleyl chitosan as dye adsorbent: Isotherms, kinetics and thermodynamic investigation. Int J Biol Macromol. 2018;117:152-66.
29. Aljeboree AM, Alrazzak NA, Alqaraguly MB, Mahdi MA, Jasim LS, Alkaim AF. Adsorption of pollutants by using low-cost (Environment-Friendly): Equilibrium, kinetics and thermodynamic studies: A review. Systematic Reviews in Pharmacy. 2020;11(12):1988-97.
30. Alshamusi QKM, Alzayd Aam, Mahdi Ma, Jasim Ls, Aljeboree Am. Adsorption of Crystal Violate (Cv) Dye In Aqueous Solutions by using P(Pvp-Co-Aam)/Go Composite as (Eco-Healthy Adsorbate Surface): Characterization and Thermodynamics Studies. Biochemical and Cellular Archives. 2021;21:2423-31.
31. Aljeboree AM, Mohammed RA, Mahdi MA, Jasim LS, Alkaim AF. Synthesis, characterization of p(Ch/aa-co-am) and adsorptive removal of pb (ii) ions from aqueous solution: Thermodynamic study. NeuroQuantology. 2021;19(7):137-43.
32. Bashir S, Teo YY, Ramesh S, Ramesh K. Physico-chemical characterization of pH-sensitive N-Succinyl chitosan-g-poly (acrylamide-co-acrylic acid) hydrogels and in vitro drug release studies. Polym Degrad Stab. 2017;139:38-54.
33. Dan S, Banivaheb S, Hashemipour H. Synthesis, characterization and absorption study of chitosan-g-poly (acrylamide-co-itaconic acid) hydrogel. Polym Bull. 2021;78(4):1887-907.